

## GENE THERAPY

# Telomerase gene therapy rescues telomere length, bone marrow aplasia, and survival in mice with aplastic anemia

Christian Bär,<sup>1</sup> Juan Manuel Povedano,<sup>1</sup> Rosa Serrano,<sup>1</sup> Carlos Benitez-Buelga,<sup>2</sup> Miriam Popkes,<sup>1</sup> Ivan Formentini,<sup>3</sup> Maria Bobadilla,<sup>4</sup> Fatima Bosch,<sup>5</sup> and Maria A. Blasco<sup>1</sup>

<sup>1</sup>Telomeres and Telomerase Group, Molecular Oncology Program and <sup>2</sup>Human Genetics Group, Spanish National Cancer Research Centre, Madrid, Spain; <sup>3</sup>Roche Pharma Research and Early Development, Neuroscience, Ophthalmology, and Rare Disease, Roche Innovation Center and <sup>4</sup>Roche Extending the Innovation Network Academia Partnering Program, F. Hoffmann-La Roche, Basel, Switzerland; and <sup>5</sup>Centre of Animal Biotechnology and Gene Therapy, Department of Biochemistry and Molecular Biology, School of Veterinary Medicine, Universitat Autònoma de Barcelona, Bellaterra, Spain

### Key Points

- Telomerase gene therapy in a mouse model of aplastic anemia targets the bone marrow and provides increased and stable telomerase expression.
- Telomerase expression leads to telomere elongation and subsequently to the reversal of aplastic anemia phenotypes.

**Aplastic anemia is a fatal bone marrow disorder characterized by peripheral pancytopenia and marrow hypoplasia. The disease can be hereditary or acquired and develops at any stage of life. A subgroup of the inherited form is caused by replicative impairment of hematopoietic stem and progenitor cells due to very short telomeres as a result of mutations in telomerase and other telomere components. Abnormal telomere shortening is also described in cases of acquired aplastic anemia, most likely secondary to increased turnover of bone marrow stem and progenitor cells. Here, we test the therapeutic efficacy of telomerase activation by using adeno-associated virus (AAV)9 gene therapy vectors carrying the telomerase *Tert* gene in 2 independent mouse models of aplastic anemia due to short telomeres (*Trf1*- and *Tert*-deficient mice). We find that a high dose of AAV9-*Tert* targets the bone marrow compartment, including hematopoietic stem cells. AAV9-*Tert* treatment after telomere attrition in bone marrow cells rescues aplastic anemia and mouse survival compared with mice treated with the empty vector. Improved survival is associated with a significant increase in telomere length in peripheral blood and bone marrow cells, as well as improved blood counts. These findings indicate that telomerase**

**gene therapy represents a novel therapeutic strategy to treat aplastic anemia provoked or associated with short telomeres. (*Blood*. 2016;127(14):1770-1779)**

## Introduction

Aplastic anemia is a potentially life-threatening, rare, and heterogeneous disorder of the blood in which the bone marrow cannot produce sufficient new blood cells due to a marked reduction of immature hematopoietic stem and progenitor cells (HSPCs).<sup>1,2</sup> The main disease manifestations are pancytopenia and marrow hypoplasia, which can emerge at any stage of life but are more frequent in young individuals (age 10-25 years) and in the elderly (>60 years).<sup>3</sup> Aplastic anemia can be acquired or inherited. The acquired type is often of idiopathic origin and involves autoimmune processes but can also be triggered by environmental factors such as exposure to radiation, toxins, and viral infections.<sup>4</sup> The congenital form is rarer, and mutations in more than 30 genes involved in DNA repair, ribosome biogenesis, and telomere maintenance pathways have been identified to date.<sup>5</sup> A frequently observed clinical feature of aplastic anemia is the presence of short telomeres in subpopulations of peripheral blood cells (neutrophils in particular; less prominent in lymphocytes),<sup>6</sup> even in the absence of mutations in the telomere maintenance machinery.

Telomeres, the termini of vertebrate chromosomes, are specialized nucleoprotein structures composed of tandem repeat sequences (TTAGGG in vertebrates) bound by a 6-protein complex (TRF1,

TRF2, TIN2, RAP1, TPP1, and POT1) known as shelterin.<sup>7,8</sup> Telomeres are essential for chromosome integrity by preventing telomere fusions and telomere fragility. Telomere length is controlled by the ribonucleoprotein enzyme telomerase, which can add telomeric sequences onto telomeres de novo. Because telomeres shorten with every cell division (a phenomenon known as the “end replication problem”) and somatic cells do not express sufficient telomerase to compensate for this, telomeres shorten throughout life. When telomeres reach a critically short length, their protective function is impaired, eliciting a persistent DNA-damage response at chromosome ends, which leads to cellular senescence or cell death.<sup>9,10</sup> Hematopoietic stem cells, in contrast to most somatic cells, can activate telomerase; however, this is insufficient to prevent telomere attrition with aging, thus eventually leading to loss of the regeneration potential of hematopoietic stem cells.<sup>11</sup> In line with this, recipients of bone marrow transplants have shorter telomeres than their donors, suggesting that telomerase cannot fully compensate for the increased cell proliferation that occurs during the engraftment phase of the transplanted bone marrow.<sup>12</sup> Telomeres also show an accelerated rate of shortening in patients with aplastic anemia compared with

Submitted August 31, 2015; accepted January 27, 2016. Prepublished online as *Blood* First Edition paper, February 22, 2016; DOI 10.1182/blood-2015-08-667485.

The online version of this article contains a data supplement.

The publication costs of this article were defrayed in part by page charge payment. Therefore, and solely to indicate this fact, this article is hereby marked “advertisement” in accordance with 18 USC section 1734.

© 2016 by The American Society of Hematology

healthy individuals, most likely due to a higher than normal number of cell divisions in the aplastic anemia cases.<sup>13</sup>

Accelerated telomere shortening due to defects in telomerase or other telomere maintenance genes prematurely limits the proliferation potential of cells, including stem cells, leading to decreased tissue renewal capacity.<sup>9,14</sup> Highly proliferative tissues such as the hematopoietic system are particularly vulnerable to defects in telomere maintenance genes, leading to severe disorders such as aplastic anemia.<sup>15</sup> As an example, the telomeropathy dyskeratosis congenita (DKC) has been linked to mutations in 11 genes that encode components of the telomerase complex (*TERT*, *TERC*, *DKC1*, *NOP10*, and *NHP2*) or of the telomere capping complex shelterin (*TIN2*). Other genes altered in DKC encode for accessory proteins important for telomerase assembly and trafficking (*CTC1*, *ACD7* [alias *TPP1*], and *TCAB1*) or for telomere replication (*RTEL1*).<sup>16</sup> Mutated *PARN* was also recently linked to reduced messenger RNA (mRNA) levels of several key genes in telomere maintenance.<sup>17</sup> In all these cases, DKC is characterized by very short telomeres. DKC is a multisystem syndrome comprising diverse clinical features such as nail dystrophy, oral leukoplakia, abnormal skin pigmentation, and cerebellar hypoplasia.<sup>16</sup> The most severe complication, however, is the development of aplastic anemia in 80% of the cases, underlining that the clinical features are caused by excessive telomere shortening that eventually leads to the exhaustion of the stem cell reserve.<sup>5</sup>

These findings suggest that telomerase activation could be a good therapeutic strategy to treat those forms of aplastic anemia associated with a limited blood-forming capacity due to the presence of very short telomeres. We have previously developed a telomerase (*Tert*) gene therapy using adeno-associated virus (AAV)9 vectors,<sup>18</sup> which attenuated or reverted aging-associated telomere erosion in peripheral blood mononuclear cells (PBMCs).<sup>18</sup>

To test the efficacy of this strategy in the treatment of aplastic anemia, we first used a mouse model of aplastic anemia generated by us in which we depleted the TRF1 shelterin protein specifically in the bone marrow, leading to a bone marrow phenotype that recapitulates the main pathological findings of human aplastic anemia patients, including extreme telomere shortening.<sup>19,20</sup> In particular, partial depletion of the *Trf1* gene specifically in bone marrow causes severe telomere uncapping and provokes a persistent DNA-damage response at telomeres, which in turn leads to a fast clearance of those HSPCs deficient for *Trf1*. In this context, the remaining HSPCs that did not delete the *Trf1* gene undergo additional rounds of compensatory proliferation to regenerate the bone marrow, leading to very rapid telomere attrition. Thus, partial depletion of the bone marrow stem cell and progenitor compartments by *Trf1* deletion recapitulates the compensatory hyperproliferation and short telomere phenotype observed after bone marrow transplant or in other acquired forms of aplastic anemia, as well as in patients due to mutations in telomere maintenance genes. Interestingly, this mouse model allows adjustment of the rate of telomere shortening by modulating the frequency of *Trf1* deletion-mediated HSPC depletion, thus controlling the onset of bone marrow aplasia and pancytopenia.<sup>19,20</sup>

As an additional model to mimic the presence of very short telomeres specifically in the bone marrow, we transplanted irradiated wild-type mice with bone marrow from late (third)-generation (G3) telomerase-deficient *Tert*-knockout mice, which have short telomeres due to telomerase deficiency during 3 mouse generations.

Here, we tested telomerase activation by using gene therapy AAV vectors in both mouse models of aplastic anemia produced by short telomeres. Our results show that telomerase treatment is sufficient to attenuate telomere attrition and HSPC depletion with time, thus significantly preventing death by bone marrow failure.

## Material and methods

### Study approval

All experimental procedures with mice (*Mus musculus*) were approved by the Spanish National Cancer Research Center Instituto de Salud Carlos III Ethics Committee for Research and Animal Welfare. Mice were treated in accordance to the Spanish laws and the Federation of European Laboratory Animal Science Associations guidelines (approval file number CBA PA 87\_2012).

### Mice and animal procedures

Mice of pure C57/BL6 background were produced and housed at the specific-pathogen-free animal house of the Spanish National Cancer Research Center in Madrid, Spain. *Trf1<sup>lox/lox</sup> Mx1-Cre* and *Trf1<sup>lox/lox</sup> Mx1-wt* mice were generated as described previously.<sup>21</sup> First-generation (G1) *Tert<sup>-/-</sup>* mice were generated by intercrossing *Tert<sup>+/-</sup>*. G3 *Tert<sup>-/-</sup>* mice were obtained by intercrossing G1 mice (to give second-generation [G2] mice) and subsequently intercrossing G2 mice.<sup>22</sup> Ten-week-old *Trf1<sup>lox/lox</sup> Mx1-Cre* or G3 *Tert<sup>-/-</sup>* mice were used as bone marrow donors for transplant into 8-week-old lethally irradiated (12 Gy) wild-type mice as described previously.<sup>19,23</sup> Two million cells were transplanted via tail vein injection at a donor-to-recipient ratio of 1:8, and mice were left for 30 days to allow bone marrow reconstitution. To induce Cre expression, mice were intraperitoneally injected with 15 µg/g body weight of polyinosinic: polycytidylic acid (pI:pC; Sigma-Aldrich) 3 times per week for a total of 5 weeks. After 1 week, mice were treated with the AAV9-*Tert* or AAV9-empty vector. Vectors were administered via tail vein injection at a concentration of  $3.5 \times 10^{12}$  viral genomes per mouse.

### Gene therapy vector production

Viral vectors were generated<sup>24</sup> and purified as described previously.<sup>25</sup> Briefly, vectors were produced through triple transfection of HEK293T. Expression cassettes were under the control of the cytomegalovirus promoter and contained an SV40 polyA signal for *EGFP* and the cytomegalovirus promoter, and a 3' untranslated region of the *Tert* gene as polyA signal for *Tert*. AAV9 particles were purified using 2 cesium chloride gradients, dialyzed against phosphate-buffered saline (PBS) and filtered.<sup>25</sup> Viral genome particle titers were determined by a quantitative real-time polymerase chain reaction (PCR) method.<sup>26</sup>

### Histology

Bone marrow samples (sternum or tibia bone) were fixed in 4% paraformaldehyde and paraffin embedded after decalcification. Tissue sections (5 µm) were stained with hematoxylin and eosin. Immunohistochemistry was performed on deparaffinized sections. After antigen retrieval, samples were stained with anti-enhanced green fluorescent protein (EGFP) (rabbit anti-EGFP, 1:200, ab290; Abcam). EGFP-positive cells were counted in a semiautomated way using ImageJ software.

### FACS

For sorting of HSPCs, whole bone marrow cells were extracted from the long bones (femur and tibia) as described previously.<sup>23</sup> Erythrocytes were lysed for 10 minutes in 10 mL of erythrocyte lysis buffer (Roche), washed once with 10 mL of PBS, and resuspended in fluorescence-activated cell sorting (FACS) buffer (PBS, 2 mM EDTA, 0.3% bovine serum albumin) containing Fc-block (1:400) at a concentration of  $5$  to  $10 \times 10^6$  cells per 100 µL. Cells were incubated for 10 minutes and washed once in FACS buffer. Cells were then resuspended in FACS buffer at  $20$  to  $25 \times 10^6$  cells per milliliter, and the antibody cocktail was added as follows: anti-Sca-1-PerCP-Cy5.5 (1:200), lin cocktail-eFluor450 (1:50) (all eBioscience), and anti-c-kit-APC-H7 (1:100) (BD Pharmingen). Cells were incubated for 30 minutes. After washing cells twice with PBS, 2 mL of 4,6 diamidino-2-phenylindole (DAPI; 2 mg/mL) was added and cells were sorted in a FACSaria IIU (Becton Dickinson, San Jose, CA) into HSPCs (lin<sup>-</sup>, Sca-1<sup>+</sup>, and c-kit<sup>+</sup>) and lineage-positive fractions.

## Colony-forming assay

A short-term colony-forming assay was performed by plating  $1 \times 10^4$  and  $2 \times 10^4$  freshly isolated mononucleated bone marrow cells in 35 mm dishes containing MethoCult media (both STEMCELL Technologies) following the manufacturer's protocol. All experiments were performed in duplicate, and the number of colonies was counted after 12 days of incubation at 37°C.

## Blood counts

Peripheral blood was drawn from the facial vein (~50  $\mu$ L) and collected into anticoagulation tubes (EDTA). Blood counts were determined using an Abacus Junior Vet veterinary hematology analyzer.

## Quantitative real-time PCR and western blot analysis

Total RNA from whole bone marrow extracts or from bone marrow cells sorted by FACS was isolated using QIAGEN's RNeasy Mini Kit according to the manufacturer. Quantitative real-time PCR was performed using an ABI PRISM 7700 or QuantStudio 6 Flex (both Applied Biosystems). Primer sequences for *Tert* and reference genes *Act1* and *TBP* are as follows: *Tert*-forward 5'GGATTGCCACTGGCTCCG; *Tert*-reverse 5'TGCCTGACCTCTCTTGTGAC; *actin*-forward 5'GGCACCACACCTTCTACAATG; *actin*-reverse 5'GTGGTGGTGAAGCTGTAG; *TBP*-forward 5'CTTCTGCCACAATGTCACAG; *TBP*-reverse 5'CCTTTCTCATGCTTGCTTCTCTG.

## Q-FISH telomere analysis

Quantitative FISH (Q-FISH) on paraffin-embedded tissue sections was performed as described previously.<sup>27</sup> Confocal images were acquired as stacks every 0.5  $\mu$ m for a total of 1.5  $\mu$ m using a Leica SP5-MP confocal microscope, and maximum projections were done with the Leica Application Suite—Advanced Fluorescence software. Telomere signal intensity was quantified in at least 6 images per mouse using Definiens software, with a specific script allowing for individual spot background correction.

High-throughput (HT)-Q-FISH on peripheral blood leukocytes was done using 120 to 150  $\mu$ L of blood as described previously.<sup>28</sup> Confocal images were captured using the Opera High-Content Screening system (Perkin Elmer). Telomere length values were analyzed using individual telomere spots (>10 000 telomere spots per sample). The average fluorescence intensities of each sample were converted into kilobases using L5178-R and L5178-S cells as calibration standards, which have stable telomere lengths of 79.7 kb and 10.2 kb, respectively.<sup>29</sup> Samples were analyzed in duplicate.

Real-time PCR–based measurement of relative telomere length was done on genomic DNA isolated from whole bone marrow samples following a previously described protocol.<sup>30,31</sup>

## Results

### AAV9-*Tert* targets bone marrow and hematopoietic stem cells

First, we tested the ability of AAV9 vectors to transduce bone marrow cells upon mouse IV injection. In particular, to determine the location and percentage of transduced cells, we first treated wild-type mice with an AAV9-EGFP reporter virus ( $3.5 \times 10^{12}$  viral genomes per mouse) via tail vein injections. We found that 2% of the BM cells were positive for EGFP upon immunohistochemistry with anti-EGFP antibodies in in middle bone sections, and this increased to 10% in bone regions adjacent to the joints, which showed the highest AAV9 transduction (Figure 1A-B). We then injected wild-type mice with the same amount of AAV9-*Tert* particles and determined *Tert* mRNA expression by quantitative real-time PCR in whole bone marrow isolates at 2 weeks and 8 months after virus injection. At 2 weeks posttreatment with the AAV9 vectors, *Tert* mRNA expression was significantly increased in the AAV9-*Tert*-treated mice compared with those treated with the AAV9-empty vector, and this increased expression was maintained up

to 8 months after the initial treatment (Figure 1C-E). In agreement with the known tropism of the AAV9 serotype, we found a stronger induction of *Tert* in organs such as heart and liver, which are preferential AAV9 targets (supplemental Figure 1, available on the Blood Web site).<sup>32</sup> We then studied *Tert* mRNA expression specifically in the blood-forming compartments of the bone marrow. To this end, we performed FACS of c-kit<sup>+</sup> and Sca-1<sup>+</sup> HSPCs and lin<sup>+</sup> lineage-committed cells. We found a significant increase in *Tert* mRNA in HSPCs (10-fold) and lineage-committed bone marrow cells (3.5-fold) in AAV9-*Tert*-treated mice compared with mice treated with the empty vector (Figure 1F-G), demonstrating that bone marrow cells, including HSPCs, are targeted by *Tert* gene therapy. Of note, the higher expression in whole bone marrow compared with isolated hematopoietic cells (HPSCs and lin<sup>+</sup> cells) could suggest that additional bone marrow cells corresponding to the stroma (ie, adipocytes) may also be infected. In this regard, we previously demonstrated that adipocytes are efficiently targeted by AAV9.<sup>33</sup> Moreover, the relative lower fold changes in *Tert* in HSPCs compared with total bone marrow may also be due to higher levels of endogenous *Tert* in HPSCs compared with whole bone marrow. As a control, AAV9-*Tert* treatment of wild-type mice did not affect the relative numbers of lineage-positive or -negative cells or the proportion of HSPCs (supplemental Figure 2). Given the increased *Tert* expression in HSPCs, we next addressed whether this affected their proliferation/colony-forming potential. To this end, we performed a colony-forming cell assay (MethoCult). We observed a significantly increased number of colonies in the bone marrow from AAV9-*Tert*-treated mice compared with those treated with the empty vector (Figure 1H).

In summary, IV injection of AAV9 vectors administered at a high dose can target *Tert* to hematopoietic cells, including HSPCs.

### AAV9-*Tert* treatment rescues survival in a mouse model of aplastic anemia

We next tested whether treatment with AAV9-*Tert* was effective in increasing survival upon induction of lethal aplastic anemia due to critically short telomeres. First, we used the conditional *Trf1* mouse model recently developed by us (*Trf1*<sup>lox/lox</sup> *Mx1-Cre* mice) in which we induce partial *Trf1* deletion specifically in the bone marrow.<sup>19</sup> To this end, we transplanted lethally irradiated wild-type mice with bone marrow isolated from *Trf1*<sup>lox/lox</sup> *Mx1-Cre* mice, followed by administration of pI:pC to induce the expression of Cre recombinase and *Trf1* deletion.<sup>19,20</sup> Genotyping confirmed that the new bone marrow solely consisted of donor cells with excisable *Trf1* (supplemental Figure 3). Thus, *Trf1*<sup>lox/lox</sup> *Mx1-Cre* mice allow study of the effects of *Trf1* depletion exclusively in the bone marrow. We previously showed that partial *Trf1* deletion in the bone marrow results in rapid death and removal of the *Trf1*-deleted cells, whereas cells that fail to delete *Trf1* undergo compensatory rounds of cell division, leading to rapid telomere shortening and replicative senescence, eventually resulting in bone marrow failure.<sup>19,20</sup>

Here, we induced *Trf1* deletion with pI:pC injections at a frequency of 3 times per week for 5 weeks, at which point these mice started to show signs of aplastic anemia.<sup>19,20</sup> One week after the last pI:pC injection, mice were treated with either the AAV9-*Tert* or AAV9-empty vector (Figure 2A). Mouse survival was monitored for 100 days after treatment with the AAV9 vectors (note: beyond 100 days after virus treatment, none of the mouse cohorts developed signs of aplastic anemia. At 120 days post-virus administration, all mice were euthanized for further analyses). Strikingly, AAV9-*Tert* treatment significantly increased survival: 87% of mice were still alive at 100 days after virus administration in the AAV9-*Tert*-treated group compared

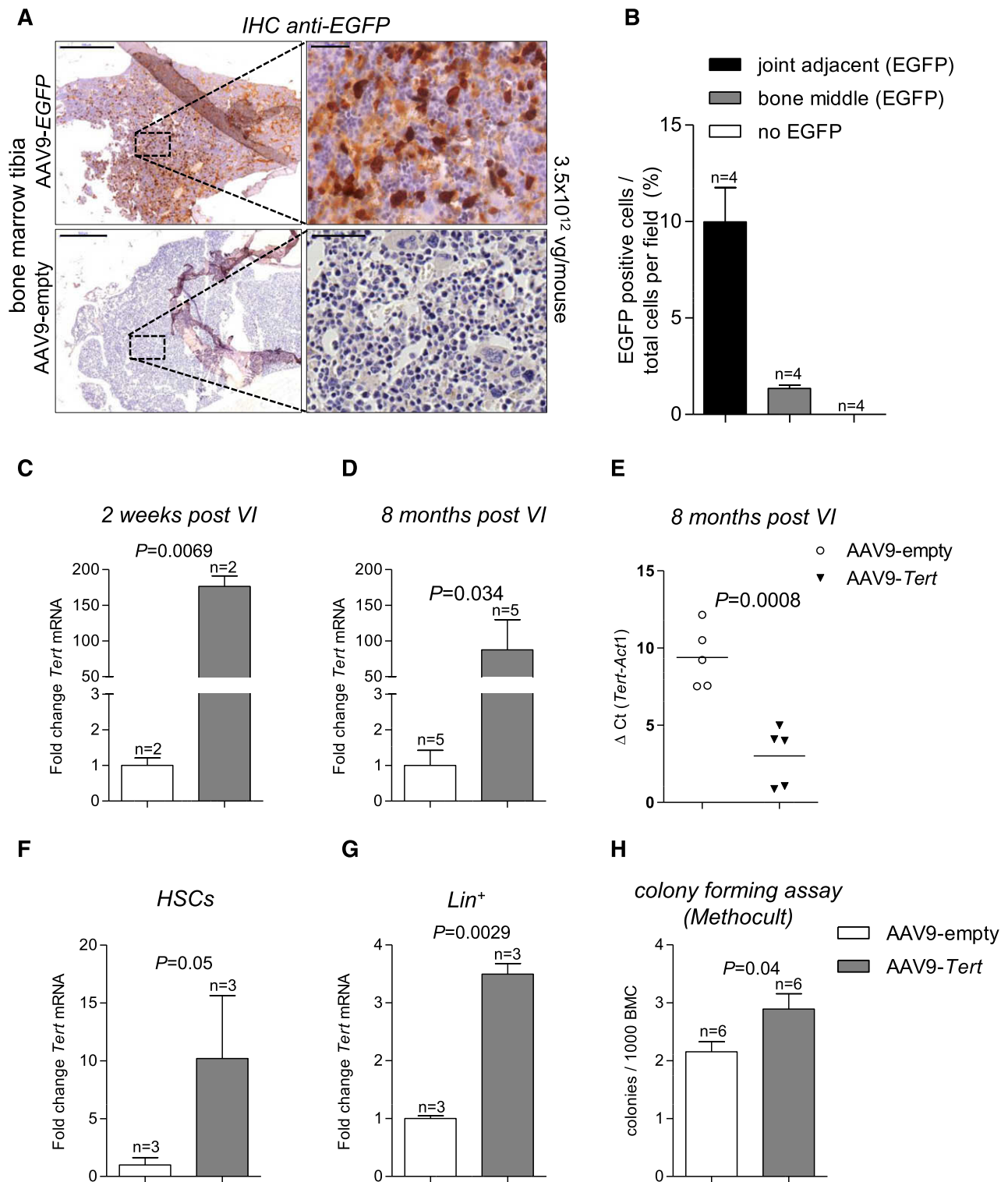


**Figure 1. High dose of AAV9 particles targets bone marrow, including HSPCs.** (A) Representative anti-EGFP immunohistochemistry (IHC) images of bone marrow corresponding to the tibia. Mice were injected with the AAV9-EGFP vector or AAV9-empty vector at a concentration of  $3.5 \times 10^{12}$  viral genomes (vg) per mouse. EGFP-positive cells were mainly located toward the end of the bones. Bars represent 500  $\mu$ m (left) and 50  $\mu$ m (right); hematoxylin and eosin stain. (B) Percentage of EGFP-positive cells relative to the total number of cells. Cells were separately counted in joint adjacent areas and in the middle of the bone. (C-D) *Tert* mRNA expression level in total bone marrow isolated 2 weeks (C) and 8 months (D) after VI with  $3.5 \times 10^{12}$  viral genomes per mouse. AAV9-*Tert* relative to the expression of mice injected with the same amount of AAV9-empty vector. (E)  $\Delta Ct$  values (*Tert* minus *Act1*) of the quantitative real-time PCR shown in panel D. Quantitative real-time PCR determined relative *Tert* expression in HSPCs (HSCs) sorted by FACS (F) and lineage-committed cells (G). (H) Colony-forming assay in MethoCult with whole bone marrow cells isolated from mice injected with AAV9-*Tert* or AAV9-empty. For all experiments, n indicates number of mice. Data are mean  $\pm$  SEM. Statistical analysis: 2-sided Student *t* test; *P* values are shown. SEM, standard error of the mean; VI, virus injection.

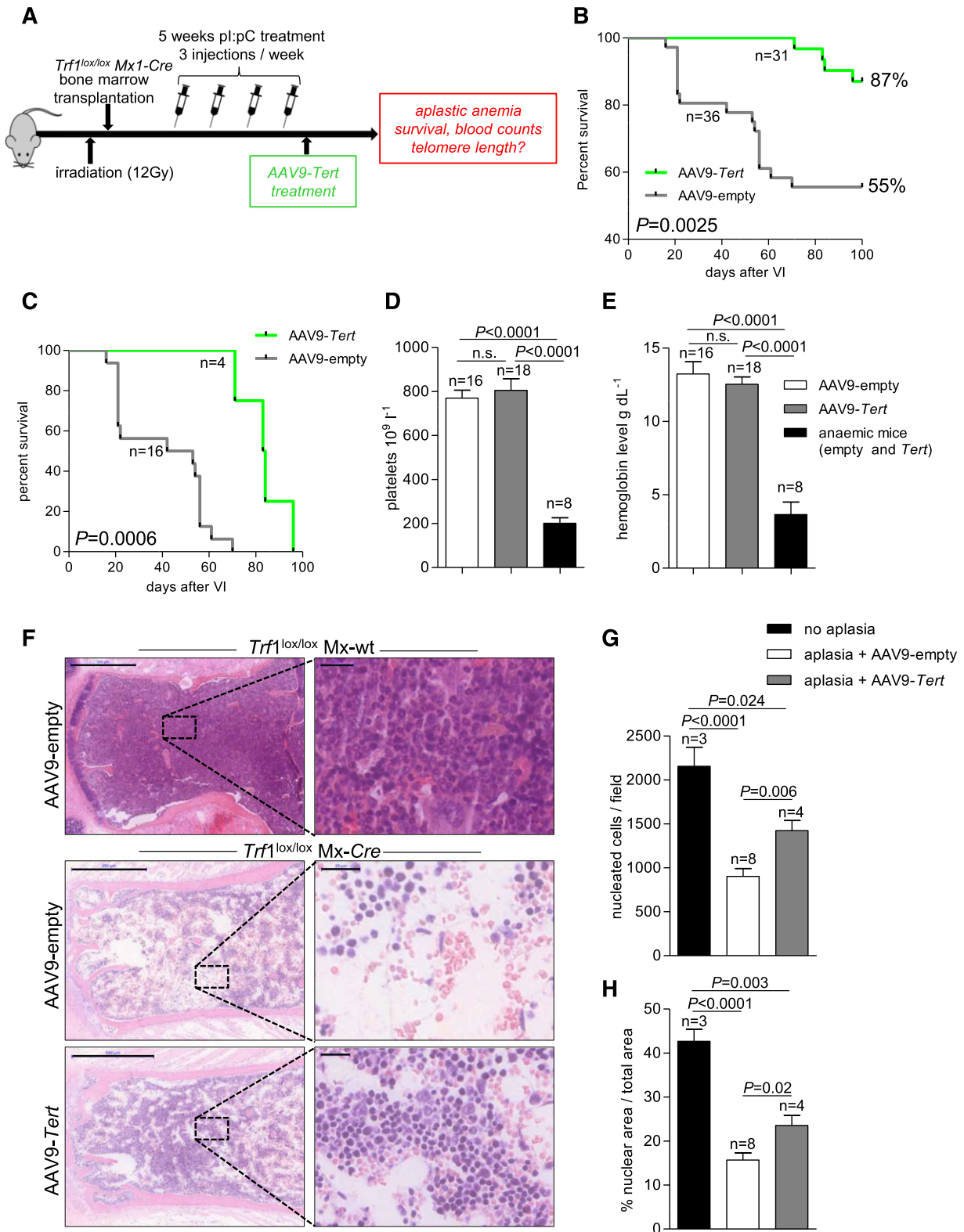


**Figure 2. AAV9-Tert treatment rescues the aplastic anemia phenotype in *Trf1*<sup>lox/lox</sup> mice.** (A) Experimental design. Mice were lethally irradiated and transplanted the following day with *Trf1*<sup>lox/lox</sup> Mx1-Cre bone marrow. After engraftment, Cre expression and *Trf1* excision was induced by pl:pC injections for 5 weeks. One week later, mice were injected with AAV9-Tert or AAV9-empty particles. (B) Kaplan-Meier survival curves showing that AAV9-Tert treatment significantly rescues mouse survival. (C) Kaplan-Meier survival curves considering only those animals that died of aplastic anemia within 100 days after virus treatment show significant protection of AAV9-Tert treatment from deaths due to aplastic anemia. Platelet counts (D) and hemoglobin levels (E) in mice of the AAV9-Tert-treated and AAV9-empty-treated groups showing clear signs of anemia compared with healthy mice from the same AAV9-Tert-treated and AAV9-empty-treated groups. (F) Representative bone marrow images of healthy controls (no Cre-mediated induction of *Trf1* deletion) and of mice with bone marrow aplasia. Genotypes and AAV9 treatments are indicated. Bars represent 500  $\mu\text{m}$  (left) and 20  $\mu\text{m}$  (right); hematoxylin and eosin stain. (G) Quantification of bone marrow cellularity expressed as number of nucleated cells per field. Four to five fields per mouse were counted. (H) Quantification of bone marrow cellularity expressed as the percentage of nuclear area (purple stain) to total areas per field. Four to five fields per mouse were counted. In all graphs, n indicates number of mice. Data are mean  $\pm$  SEM. Statistical analysis: log-rank test in panels B and C; 2-sided Student *t* test in panels D, E, G, and H; *P* values are shown. n.s., not significant.

with only 55% of mice alive in the empty vector–treated group (Figure 2B). In particular, whereas only 4 of 31 mice (13%) treated with AAV9-*Tert* developed aplastic anemia, 16 of 36 mice (44%) died with clear signs of aplastic anemia in the group treated with the empty vector (Figure 2C). In both groups, aplastic anemia was determined as the cause of death in those mice showing a drastic drop in platelet counts and hemoglobin levels at the time of death (Figure 2D-E) and presenting with severe bone marrow hypoplasia and aplasia after postmortem histopathological analysis of bone marrow sections (Figure 2F). Interestingly, among those mice that died of aplastic anemia, we observed a tendency to show a milder bone marrow aplasia phenotype in the AAV9-*Tert*-treated group compared with the AAV9-empty-treated group, as indicated by higher bone marrow cellularity in the AAV9-*Tert*-treated group (Figure 2F). Quantification of the bone marrow cellularity confirmed a drastic decrease of cellularity in aplastic anemia mice compared with wild-type control mice. Of importance, the decrease in cellularity was significantly attenuated in the AAV9-*Tert*-treated cohort compared with the AAV9-empty-treated group (Figure 2G-H). Our results suggest that AAV9-*Tert* treatment of mice with induced severe telomere shortening significantly reduces mortality due to aplastic anemia.

#### Telomerase treatment reverses telomere shortening in peripheral blood and bone marrow cells in a mouse model of aplastic anemia

Because aplastic anemia in our mouse model is caused by extreme telomere shortening,<sup>19,20</sup> we next compared the dynamics of telomere length in mice treated with AAV9-*Tert* vs mice treated with the empty vector. To this end, we performed a longitudinal study to follow telomere length in peripheral blood (PBMCs) over time using telomere HT-Q-FISH technology.<sup>34</sup> To do so, we extracted blood at 4 different time points (time point 1, 30 days after bone marrow engraftment; time point 2, 5 weeks after pI:pC treatment; time point 3, 2 months after treatment with the AAV9 vectors; and time point 4, 4 months after treatment with the AAV9 vectors) (note: longitudinal telomere measurements were done on PBMCs from mice that did not develop aplastic anemia). In agreement with previous findings, we found a dramatic drop in telomere length of ~10 kb in all mice after induction of *Trf1* deletion with pI:pC and prior to treatment with the gene therapy vectors (Figure 3A; compare time points 1 and 2).<sup>19,20</sup> We observed a further drop in telomere length in those mice treated with the AAV9-empty vector when comparing time point 4 with time point 2 in this mouse cohort (Figure 3A-B). Importantly, during the same period of time, mice treated with AAV9-*Tert* showed a net increase in average telomere length of 10 kb when comparing time point 4 with time point 2 (Figure 3A-B). Indeed, throughout the course of the experiment, AAV9-empty-treated mice showed a total decrease in average telomere length of 12 kb, whereas mice treated with AAV9-*Tert* showed re-elongation of telomeres to a similar telomere length as before the induction of *Trf1* deletion by pI:pC treatment (Figure 3C). These findings indicate that AAV9-*Tert* treatment is sufficient to stop and even revert initial telomere shortening. To further confirm whether telomeres were elongated as the consequence of AAV9-*Tert* gene therapy specifically in the bone marrow, we performed Q-FISH analysis on bone marrow cross-sections at the end point of the experiment. In agreement with longer telomeres in peripheral blood cells in the AAV9-*Tert*-treated mice, we found that AAV9-*Tert*-treated mice also had significantly longer telomeres in the bone marrow compared with mice treated with the empty vector (Figure 3D-F). We confirmed the AAV9-*Tert*-mediated telomere elongation on independent samples using a real-time PCR

assay for relative telomere length determination<sup>30,31</sup> (supplemental Figure 4A). Furthermore, in line with our hypothesis that aplastic anemia is the consequence of drastically shortened telomeres, mice treated with the AAV9-empty vector that developed aplastic anemia had significantly shorter telomeres than mice that were treated in the same manner but did not develop aplastic anemia (supplemental Figure 4B).

Of note, telomere length analysis on bone marrow sections or bone marrow DNA does not allow one to distinguish between various cell populations. However, the observed telomere elongation in PBMCs suggests a direct effect of AAV9-*Tert* on HSPCs.

#### Telomerase gene therapy of aplastic anemia produced by short telomeres resulting from *Tert* deletion improves blood counts and increases telomere length

To validate the therapeutic use of telomerase gene therapy in aplastic anemia provoked by short telomeres, we used an additional mouse model for modeling short telomere length in the hematopoietic system (in this case due to telomerase deficiency during several mouse generations): the *Tert*-deficient mouse model.<sup>22</sup> To this end, we irradiated wild-type mice and transplanted them with bone marrow from G3 *Tert*-knockout mice, which have short telomeres in all mouse tissues, including the bone marrow<sup>22</sup> (Figure 4A). First, we confirmed shorter telomeres in the G1 and G3 *Tert*-knockout bone marrow donors compared with the wild-type bone marrow donors by performing HT-Q-FISH analysis on PBMCs. In particular, *Tert* deficiency leads to progressive telomere shortening, with G3 mice having an average telomere length of ~25 kb compared with ~40 kb in the wild-type controls (Figure 4B). One month after transplantation of irradiated wild-type mice with G3 *Tert* knockout bone marrow, mice were divided in 2 groups and treated with either AAV9-*Tert* or AAV9-empty gene therapy vectors ( $3.5 \times 10^{12}$  viral genomes per mouse) (Figure 4A). After treatment, we monitored mice during a follow-up period of 5 months and observed robust expression of *Tert* in the bone marrow in the AAV9-*Tert*-treated group (supplemental Figure 5). Importantly, in response to AAV9-*Tert* treatment, we observed an increase in survival compared with the AAV9-empty-treated group that almost reached statistical significance ( $P = .058$ ) (Figure 4C). Upon mouse euthanasia, *Tert*-treated mice had significantly increased hemoglobin levels and higher erythrocyte and platelet counts compared with mice treated with the empty vector (Figure 4D-F). The same trend was observed for leukocyte counts, which were higher in AAV9-*Tert*-treated mice compared with the AAV9-empty group, although the trend did not reach statistical significance ( $P = .09$ ) (Figure 4G). Lastly, to analyze the mechanism by which *Tert* gene therapy improved survival and blood counts in these mice, we followed longitudinally the telomere length in PBMCs in both mouse cohorts. To this end, we extracted blood before and 3 and 5 months after mice were injected with the viruses and performed HT-Q-FISH analysis. In line with the results obtained with the *Trf1*<sup>lox/lox</sup> mouse model (see “AAV9-*Tert* treatment rescues survival in a mouse model of aplastic anemia”), we found that AAV9-*Tert* treatment led to a net increase in average telomere length of 5.18 kb with time, whereas during the same period, mice treated with the AAV9-empty vector suffered a slight telomere shortening of -1.76 kb (Figure 5A-B). These findings were also confirmed by telomere Q-FISH analysis on bone marrow sections at 5 months after virus administration. In particular, we found significantly longer telomeres in the bone marrow of *Tert*-treated mice compared with mice treated with the empty vector (Figure 5C-D).

In summary, these results indicate that a single treatment with the AAV9-*Tert* vector in mice with previously shortened telomeres in the bone marrow due to telomerase deficiency is sufficient to increase

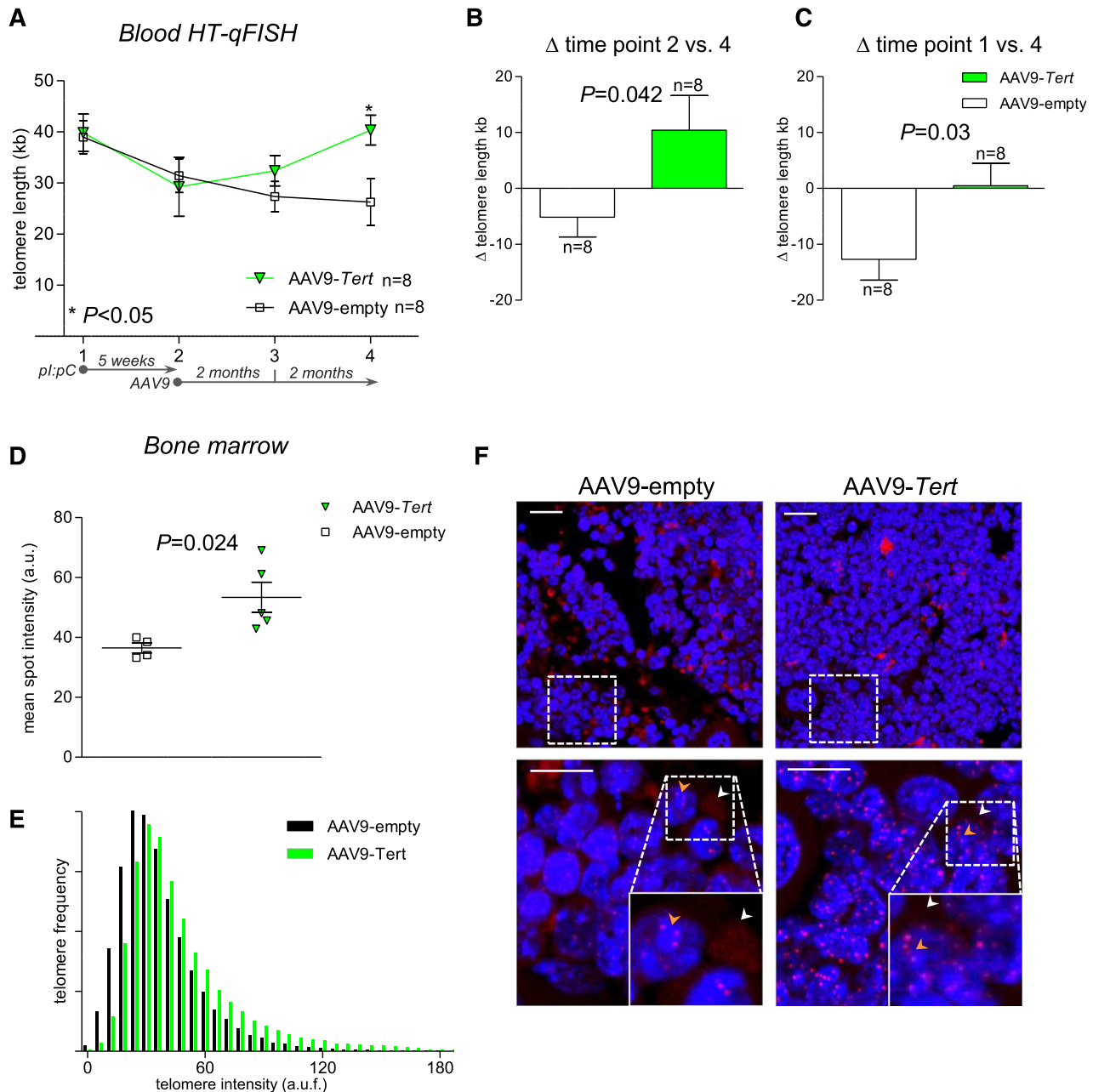


**Figure 3. AAV9-*Tert* treatment causes telomere elongation in blood and bone marrow.** (A) Longitudinal HT-Q-FISH analysis of telomere length in peripheral blood monocytes (*Trf1*<sup>lox/lox</sup> *Mx1-Cre*-transplanted mice; see also Figure 2A). Blood was extracted at 4 different time points (time point 1, before pl:pC treatment; time point 2, after 5 weeks of pl:pC treatment and before AAV9 injection; time point 3, 2 months after AAV9 injection; and time point 4, 4 months after AAV9 injection). Relative variation ( $\Delta$ ) of telomere length in AAV9-*Tert*-treated and AAV9-empty-treated animals between time points 2 and 4 (B) and between time points 1 and 4 (C). (D) Relative telomere length in bone marrow sections from AAV9-*Tert*-treated and AAV9-empty-treated mice shown as arbitrary units of fluorescence (a.u.f.). Each square and triangle represents the mean telomere length per nucleus of an individual mouse. (E) Frequency distribution blot of telomere length showing a higher abundance of short telomeres in the AAV9-empty-treated group compared with AAV9-*Tert*-treated mice (pooled data from panel D). (F) Representative images of bone marrow sections from AAV9-*Tert*-treated and AAV9-empty-treated mice used for Q-FISH analysis. Cell nuclei are stained blue (DAPI) and telomeres are stained red (Cy3). White arrowheads indicate nonspecific extranuclear signals and yellow arrowheads indicate specific telomere signals within DAPI-stained nuclei. Bars represent 20  $\mu$ m (top) and 10  $\mu$ m (bottom). In all graphs, n indicates number of mice. Data are mean  $\pm$  SEM. Statistical analysis: 2-way analysis of variance in panel A; 2-sided Student *t* test in panels B and C; *P* values are shown. a.u., arbitrary units.

telomere length in the bone marrow and in blood. Telomerase gene therapy also improved blood counts and mouse survival.

## Discussion

Here, we set out to test the hypothesis of whether increased expression of telomerase through systemic virus-based *Tert* delivery may delay or

prevent the emergence of aplastic anemia provoked by short telomeres. We tested this hypothesis in 2 independent mouse models with very short telomeres specifically in the bone marrow due to either *Trf1* or *Tert* deficiency.<sup>20,22</sup>

The rationale for this study was based on our previous finding showing that systemic AAV9-*Tert* gene therapy in wild-type mice was sufficient to delay different age-related diseases and to significantly increase mouse life span by delaying telomere shortening with age in different tissues.<sup>18</sup> A 5-month longitudinal follow-up of these mice also

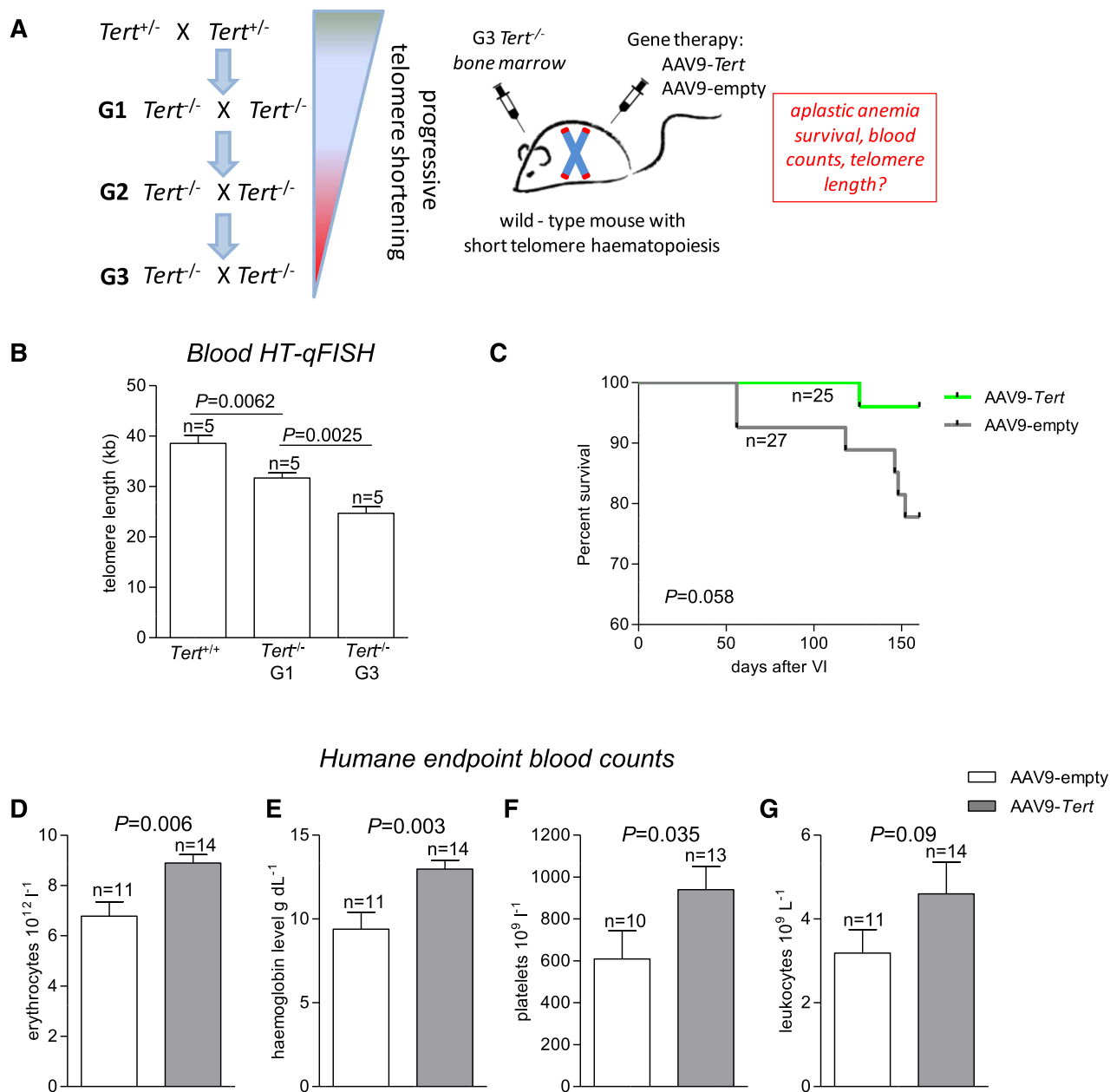


**Figure 4. AAV9-*Tert* treatment improves blood counts in mice with short telomeres resulting from specific *Tert* deletion in the bone marrow.** (A) Experimental design. G3  $Tert^{-/-}$  mice with short telomeres were generated by consecutive crosses of *Tert*-deficient mice. Bone marrow from these G3 mice was isolated and transplanted into irradiated wild-type mice. After engraftment, mice were injected with AAV9-*Tert* or AAV9-empty virus particles. (B) HT-Q-FISH analysis of telomere length in PBMCs from wild-type, G1  $Tert^{-/-}$ , and G3  $Tert^{-/-}$  mice reveals progressive telomere shortening with consecutive mouse generations. (C) Kaplan-Meier survival curves show that AAV9-*Tert* treatment improves survival of mice with very short telomeres in the bone marrow due to *Tert* deficiency specifically in the bone marrow (irradiated wild-type mice transplanted with G3  $Tert^{-/-}$  bone marrow). AAV9-*Tert* compared with AAV9-empty treatment improves erythrocyte counts (D), hemoglobin levels (E), platelet counts (F), and leukocyte counts (G). In all graphs, n indicates number of mice. Data are mean  $\pm$  SEM. Statistical analysis: log-rank test in panel A; 2-sided Student *t* test in panels B and E-H; *P* values are shown.

revealed increased telomere length in PBMCs from mice treated with telomerase gene therapy, suggesting that the vectors were also targeting the bone marrow.<sup>18</sup> This finding is in line with recent reports showing that AAV9 viral genome copies are readily detectable in bone marrow isolates even 20 weeks postinjection<sup>35</sup> and with the fact that FACS analysis of bone marrow from neonatal mice administered AAV9-green fluorescent protein show increased amounts of green fluorescent protein-positive cells.<sup>36</sup> Thus, *Tert* delivery via AAV9 may hold potential for treating aplastic anemia triggered or associated with short telomeres in the bone marrow, a common consequence of telomerase

mutations in the so-called telomeropathies or telomere syndromes, as well as in some acquired cases of aplastic anemia.<sup>37-39</sup>

To demonstrate this, we first confirmed that a high dose ( $3.5 \times 10^{12}$  viral genomes per mouse) of AAV9-EGFP reporter vector injected IV was able to transduce the bone marrow, as indicated by the presence of EGFP-positive cells. Furthermore, administration of the same amount of AAV9-*Tert* particles led to robust *Tert* expression in whole bone marrow isolates 2 weeks after treatment; this increased expression was maintained at 8 months posttreatment. To rule out the possibility that AAV9 may be targeting only bone marrow stroma cells, we

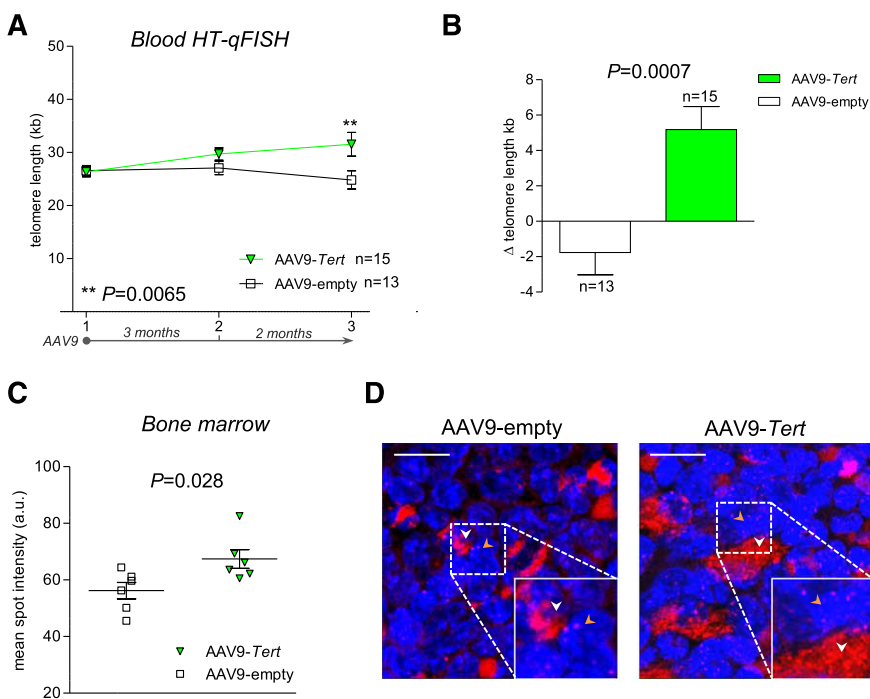


**Figure 5. Telomerase gene therapy leads to telomere elongation in peripheral blood and bone marrow cells from mice with specific deletion of *Tert* in the bone marrow.** (A) Longitudinal HT-Q-FISH analysis of telomere length in PBMCs of irradiated wild-type mice transplanted with bone marrow from G3 *Tert*<sup>-/-</sup> mice (see also Figure 4A). Blood was extracted at 3 different time points (time point 1, after G3 *Tert*<sup>-/-</sup> bone marrow engraftment and before AAV9 injection; time point 2, 3 months after AAV9 injection; and time point 3, 5 months after AAV9 injection). (B) Relative variation ( $\Delta$ ) of telomere length in AAV9-*Tert*-treated and AAV9-empty-treated animals between time points 1 and 3. (C) Telomere Q-FISH analysis on bone marrow sections from animals transplanted with G3 *Tert*<sup>-/-</sup> bone marrow and treated with AAV9-empty or AAV9-*Tert* for 5 months before euthanasia. Each square or triangle represents the mean telomere length per nucleus (expressed as arbitrary units of fluorescence) of an individual mouse. (D) Representative images of bone marrow sections from AAV9-*Tert*-treated and AAV9-empty-treated mice used for Q-FISH analysis. Cell nuclei are stained blue (DAPI) and telomeres are stained red (Cy3). White arrowheads indicate nonspecific extranuclear signals and yellow arrowheads indicate specific telomere signals within DAPI-stained nuclei. Bars represent 10  $\mu$ m. For all experiments, n indicates number of mice. Data are mean  $\pm$  SEM. Statistical analysis: 2-way analysis of variance in panel A; 2-sided Student *t* test in panels B and C; *P* values are shown.

demonstrated significantly increased *Tert* mRNA expression both in isolated hematopoietic stem cells (*lin*<sup>-</sup>, *Sca-1*<sup>+</sup>, *c-kit*<sup>+</sup>) and in lineage-committed bone marrow cells (*lin*<sup>+</sup>) from mice treated with AAV9-*Tert* compared with mice treated with the AAV9-empty vector. Importantly, bone marrow cells from AAV9-*Tert*-treated mice showed enhanced colony-forming abilities, suggesting that telomerase expression may increase the stem cell reserve.

Indeed, AAV9-*Tert* treatment of mice with aplastic anemia triggered by short telomeres resulting from marrow-specific *Trf1* deletion<sup>19</sup> significantly rescued mortality due to aplastic anemia, concomitant with telomere re-elongation in blood and bone marrow cells from these mice after telomerase treatment. We confirmed these findings by generating a second mouse model of aplastic anemia produced by short telomeres, in this case due to telomerase deficiency. In particular, we generated mice with *Tert* deficiency specifically in the bone marrow. In this case, the treatment of *Tert* gene therapy in mice with *Tert*-deficient bone marrow and short telomeres (irradiated wild-type mice transplanted with G3 *Tert*-knockout bone marrow) showed a moderate improvement of survival, which was not as dramatic as in the case of the *Trf1*-deficient bone marrow model. This result is likely due to the fact that in contrast to the *Trf1*-deletion model, which shows a very severe and rapid induction of aplastic anemia,<sup>19,20</sup> *Tert* deficiency leads to a variable penetrance of aplastic anemia with increasing mouse generations.<sup>40,41</sup> Similarly to the *Trf1*-deficient mouse model, *Tert* gene therapy of the *Tert*-deficient bone marrow mouse model also resulted in increased telomere length with time in peripheral blood cells and significantly improved blood counts. In both mouse models, improvement of blood counts can be interpreted as the consequence of improved stem cell reserve. This is in line with recently published data showing that genetic *Tert* re-activation in fifth-generation *Tert*<sup>-/-</sup> mice using a Cre-inducible system restored HSPC proliferation, concomitant with improved erythrocyte counts and hemoglobin levels.<sup>42</sup>

In summary, we provide proof of concept for a therapeutic effect of telomerase treatment using AAV9 gene therapy vectors in the treatment of aplastic anemia provoked by short telomeres. A strategy based on AAV9-*Tert* treatment may be beneficial not only in the correction of

monogenic bone marrow disease such as in carriers of *Tert* mutations (we demonstrated improved blood counts in *Tert*-knockout mice) but also in other forms of aplastic anemia associated with short telomeres and hematopoietic stem cell depletion (eg, Fanconi anemia<sup>43</sup>). Generally, due to an excellent safety profile attributable to their low immunogenicity and the fact that they are nonintegrative, AAV vectors have become an attractive gene therapy tool, and many clinical trials using those vectors are already underway (see [www.clinicaltrials.gov](http://www.clinicaltrials.gov)). However, despite the fact that AAV9 vectors carrying the *Tert* gene are nonintegrative and therefore unlikely to aid in the division of cancer cells, the association of many cancers with telomerase expression imposes specific safety concerns. In this regard, it is important to point out that in a previous study, a longer than 1-year follow-up of wild-type mice treated with AAV9-*Tert* did not show increased cancer; in fact, cancer onset was delayed in the same manner as other age-related diseases.<sup>18</sup> Nevertheless, subsequent studies should address the safety of this strategy in long-lived mammals such as primates. If those studies confirm our proof-of-principle findings, this gene therapy approach may also be adapted to treat hereditary forms of aplastic anemia caused by mutations other than *Tert* by replacing the gene to be delivered.

## Acknowledgments

This study was funded by the Spanish Ministry of Economy and Competitiveness, the Fundación Botín, and the Roche Extending the Innovation Network Academia Partnering Program (M.A.B.).

## Authorship

Contribution: M.A.B. conceived the original idea; M.A.B. and C.B. designed the experiments and wrote the paper; C.B. performed the majority of the experiments; R.S. performed the bone marrow

transplants and monitored the mice during all animal procedures; J.M.P., M.P., and C.B.-B. performed the experiments during the revision process; I.F. and M.B. contributed to scientific discussions and the experimental design; and F.B. provided the viral vectors.

**Conflict-of-interest disclosure:** The authors declare no competing financial interests.

The current affiliation for C.B. is Institute of Molecular and Translational Therapeutic Strategies, Hannover Medical School, Hannover, Germany.

**Correspondence:** Maria A. Blasco, Spanish National Cancer Research Center, Melchor Fernández Almagro 3, Madrid E-28029, Spain; e-mail: mblasco@cni.es.

## References

- Scopes J, Bagnara M, Gordon-Smith EC, Ball SE, Gibson FM. Haemopoietic progenitor cells are reduced in aplastic anaemia. *Br J Haematol*. 1994;86(2):427-430.
- Maciejewski JP, Anderson S, Katevas P, Young NS. Phenotypic and functional analysis of bone marrow progenitor cell compartment in bone marrow failure. *Br J Haematol*. 1994;87(2):227-234.
- Marsh JC, Ball SE, Cavenagh J, et al; British Committee for Standards in Haematology. Guidelines for the diagnosis and management of aplastic anaemia. *Br J Haematol*. 2009;147(1):43-70.
- Nakao S. Immune mechanism of aplastic anemia. *Int J Hematol*. 1997;66(2):127-134.
- Dokal I, Vulliamy T. Inherited bone marrow failure syndromes. *Haematologica*. 2010;95(8):1236-1240.
- Brümmendorf TH, Maciejewski JP, Mak J, Young NS, Lansdorp PM. Telomere length in leukocyte subpopulations of patients with aplastic anemia. *Blood*. 2001;97(4):895-900.
- Blackburn EH. Switching and signaling at the telomere. *Cell*. 2001;106(6):661-673.
- de Lange T. Shelterin: the protein complex that shapes and safeguards human telomeres. *Genes Dev*. 2005;19(18):2100-2110.
- Harley CB, Futcher AB, Greider CW. Telomeres shorten during ageing of human fibroblasts. *Nature*. 1990;345(6274):458-460.
- Flores I, Canela A, Vera E, Tejera A, Cotsarelis G, Blasco MA. The longest telomeres: a general signature of adult stem cell compartments. *Genes Dev*. 2008;22(5):654-667.
- Hiyama E, Hiyama K. Telomere and telomerase in stem cells. *Br J Cancer*. 2007;96(7):1020-1024.
- Wynn RF, Cross MA, Hatton C, et al. Accelerated telomere shortening in young recipients of allogeneic bone-marrow transplants. *Lancet*. 1998;351(9097):178-181.
- Ball SE, Gibson FM, Rizzo S, Tooze JA, Marsh JC, Gordon-Smith EC. Progressive telomere shortening in aplastic anemia. *Blood*. 1998;91(10):3582-3592.
- Flores I, Cayuela ML, Blasco MA. Effects of telomerase and telomere length on epidermal stem cell behavior. *Science*. 2005;309(5738):1253-1256.
- Vulliamy T, Marrone A, Dokal I, Mason PJ. Association between aplastic anaemia and mutations in telomerase RNA. *Lancet*. 2002;359(9324):2168-2170.
- Dokal I. Dyskeratosis congenita. *Hematology Am Soc Hematol Educ Program*. 2011;2011:480-486.
- Tummala H, Walne A, Collopy L, et al. Poly(A)-specific ribonuclease deficiency impacts telomere biology and causes dyskeratosis congenita. *J Clin Invest*. 2015;125(5):2151-2160.
- Bernardes de Jesus B, Vera E, Schneeberger K, et al. Telomerase gene therapy in adult and old mice delays aging and increases longevity without increasing cancer. *EMBO Mol Med*. 2012;4(8):691-704.
- Beier F, Foronda M, Martínez P, Blasco MA. Conditional TRF1 knockout in the hematopoietic compartment leads to bone marrow failure and recapitulates clinical features of dyskeratosis congenita. *Blood*. 2012;120(15):2990-3000.
- Bär C, Huber N, Beier F, Blasco MA. Therapeutic effect of androgen therapy in a mouse model of aplastic anemia produced by short telomeres. *Haematologica*. 2015;100(10):1267-1274.
- Martínez P, Thanassoulas M, Muñoz P, et al. Increased telomere fragility and fusions resulting from TRF1 deficiency lead to degenerative pathologies and increased cancer in mice. *Genes Dev*. 2009;23(17):2060-2075.
- Liu Y, Snow BE, Hande MP, et al. The telomerase reverse transcriptase is limiting and necessary for telomerase function in vivo. *Curr Biol*. 2000;10(22):1459-1462.
- Samper E, Fernández P, Eguía R, et al. Long-term repopulating ability of telomerase-deficient murine hematopoietic stem cells. *Blood*. 2002;99(8):2767-2775.
- Matsushita T, Elliger S, Elliger C, et al. Adeno-associated virus vectors can be efficiently produced without helper virus. *Gene Ther*. 1998;5(7):938-945.
- Ayuso E, Mingozzi F, Montane J, et al. High AAV vector purity results in serotype- and tissue-independent enhancement of transduction efficiency. *Gene Ther*. 2010;17(4):503-510.
- Ayuso E, Blouin V, Lock M, et al. Manufacturing and characterization of a recombinant adeno-associated virus type 8 reference standard material. *Hum Gene Ther*. 2014;25(11):977-987.
- Samper E, Goytisolo FA, Slijepcevic P, van Buul PP, Blasco MA. Mammalian Ku86 protein prevents telomeric fusions independently of the length of TTAGGG repeats and the G-strand overhang. *EMBO Rep*. 2000;1(3):244-252.
- Canela A, Klatt P, Blasco MA. Telomere length analysis. *Methods Mol Biol*. 2007;371:45-72.
- McIlrath J, Bouffler SD, Samper E, et al. Telomere length abnormalities in mammalian radiosensitive cells. *Cancer Res*. 2001;61(3):912-915.
- Cawthon RM. Telomere measurement by quantitative PCR. *Nucleic Acids Res*. 2002;30(10):e47.
- Callicott RJ, Womack JE. Real-time PCR assay for measurement of mouse telomeres. *Comp Med*. 2006;56(1):17-22.
- Inagaki K, Fuess S, Storm TA, et al. Robust systemic transduction with AAV9 vectors in mice: efficient global cardiac gene transfer superior to that of AAV8. *Mol Ther*. 2006;14(1):45-53.
- Jimenez V, Muñoz S, Casana E, et al. In vivo adeno-associated viral vector-mediated genetic engineering of white and brown adipose tissue in adult mice. *Diabetes*. 2013;62(12):4012-4022.
- Canela A, Vera E, Klatt P, Blasco MA. High-throughput telomere length quantification by FISH and its application to human population studies. *Proc Natl Acad Sci USA*. 2007;104(13):5300-5305.
- Huang J, Li X, Coelho-dos-Reis JG, Wilson JM, Tsuji M. An AAV vector-mediated gene delivery approach facilitates reconstitution of functional human CD8<sup>+</sup> T cells in mice. *PLoS One*. 2014;9(2):e88205.
- Mattar CN, Wong AM, Hoefer K, et al. Systemic gene delivery following intravenous administration of AAV9 to fetal and neonatal mice and late-gestation nonhuman primates. *FASEB J*. 2015;29(9):3876-3888.
- Armanios M, Blackburn EH. The telomere syndromes. *Nat Rev Genet*. 2012;13(10):693-704.
- Calado RT, Young NS. Telomere diseases. *N Engl J Med*. 2009;361(24):2353-2365.
- Kirwan M, Dokal I. Dyskeratosis congenita, stem cells and telomeres. *Biochim Biophys Acta*. 2009;1792(4):371-379.
- Herrera E, Samper E, Blasco MA. Telomere shortening in mTRF<sup>-/-</sup> embryos is associated with failure to close the neural tube. *EMBO J*. 1999;18(5):1172-1181.
- Herrera E, Samper E, Martín-Caballero J, Flores JM, Lee HW, Blasco MA. Disease states associated with telomerase deficiency appear earlier in mice with short telomeres. *EMBO J*. 1999;18(11):2950-2960.
- Raval A, Behbehani GK, Nguyen XT, et al. Reversibility of defective hematopoiesis caused by telomere shortening in telomerase knockout mice. *PLoS One*. 2015;10(7):e0131722.
- Dokal I, Vulliamy T. Inherited aplastic anaemias/bone marrow failure syndromes. *Blood Rev*. 2008;22(3):141-153.